

The peculiarities of implanted deuterium capture in Kh16N15M3T1 austenitic steel with different structure

G A Raspopova¹, V A Arbuzov¹

¹Institute of Metal Physics, Ural Branch of Russian Academy of Sciences, 18 Kovalevskaya str., Ekaterinburg, 620990, Russia

E-mail: raspopova@imp.uran.ru

Abstract. The results of studying of implanted hydrogen (deuterium) capture in austenitic steel Kh16N15M3T1 are reported. The peculiarities and possibilities of using the nuclear reactions method for measuring deuterium capture are discussed. The traps of implanted atoms and their capture by the elements of steel structure under radiation damage are considered. It is shown that the segregation intensity depends on the initial structure of the samples. A method is proposed for separating the contribution from different types of traps – structure elements – to implanted deuterium capture in irradiated volume. The mechanism of formation and evolution of radiation-induced segregation is discussed.

1. Introduction

As is known, the solubility of hydrogen in steels is very small. This causes embrittlement of articles made thereof that are used in hydrogen-containing atmosphere. If it is possible to block hydrogen in numerous isolated areas of the bulk (traps), the critical conditions of nucleation and development of pores and cracks can be changed. In unirradiated material, such traps are created in the form of precipitates of second phases, and under irradiation – as large density of radiation-induced hydrogen traps. The larger amount of hydrogen can be captured by these traps, the more effective they are. This problem is topical also for materials exposed to neutron irradiation, since radiation-induced nuclear reactions and corrosion processes result in a large concentration of hydrogen (up to 0.4 at. %) in parts made of austenitic steels after their long-term operation in reactors [1].

The behavior of hydrogen in fusion materials is usually examined with the use of hydrogen isotope – deuterium. Materials are saturated with deuterium either from gaseous phase or by implantation, and capture is measured by thermal desorption or by nuclear reactions. In the latter case, in situ analysis can be performed.

In this paper, the results of works [2 - 4] devoted to implanted deuterium capture in austenitic steel Kh16N15M3(T1) in different structural states, as well as the original findings are presented.

2. Materials and methods

2.1. Steel Kh16N15M3T1.

In this work we used specially prepared samples of Kh16N15M3(T1) steels with pre-assigned structure. Titanium-free and titanium-containing steels are designated as ss01 and ss11. Both steels contain (wt. %) 15.9 Cr; 15.0 Ni; 2.53 Mo and 0.03 C. Steel Kh16N15M3T1 contains also 1.02 wt. % Ti.



The samples in different structural states were prepared under the following conditions: hardening (without symbolic notation) – heating to 1373 K, 1 h exposure; deformation (**d**) – rolling of hardened samples at room temperature until 30 % deformation; annealing (**do**) – heating of cold-worked samples to 650 K and exposure at this temperature for 1 h. The sample ss11x was prepared from titanium-containing steel, which was aged upon hardening at 923 K for 20 h (**x**).

The choice of cold deformation and annealing conditions is explained by the following reasons:

1. 30% deformation degree provides for 10^{10} - 10^{11} cm⁻² dislocation density that is realized during standard deformation of austenitic steels.

2. The post-deformation annealing temperature of 650 K is sufficient for complete annealing of deformation vacancies (DV) [5], but it does not lead to considerable variation of the dislocation density.

The examined samples have the following structural peculiarities and possible initial hydrogen traps.

All the samples contain inclusions of metallurgical origin, namely, complex calcium oxides and other deoxidizing agents. Only some fragments of large inclusions in titanium-containing steels turned out to be carbides TiC that did not dissolve during heating for hardening (<<0.007 vol. %). No other precipitates were found in the hardened samples.

Particles of Ni₃Ti intermetallic or γ' -phase. Besides nonmetallic inclusions typical of hardened sample, the aged sample was found to contain ~2 vol. % small (~6 nm) particles of Ni₃Ti intermetallic. In the strained steel samples, besides nonmetallic inclusions of metallurgical origin, no other particles were found either in dislocations or outside them. However this result obtained by TEM analysis with the use of dark-field images and microdiffraction does not allow one to completely exclude the existence of very small deformation-induced [18] coherent precipitates or pre-precipitates of deformation-induced Ni₃Ti.

Dislocation structure. The TEM analysis showed that the unstrained samples contained only single dislocations that are distributed rather uniformly. Their density is $\sim 1 \cdot 10^7$ cm⁻². According to data [2], such dislocations are not effective traps of implanted deuterium.

The TEM analysis for strained samples of steel revealed that their dislocation structure has a network-cellular character. The cell size is 0.2...0.4 μ m and the average dislocation density in the samples is $\sim 3.4 \times 10^{10}$ cm⁻². Deformation twins and stacking faults are observed on the background of the network-cellular substructure in all the samples.

In the process of post-deformation annealing, the dislocation structure changes only slightly. So, the measured average cell size in annealed sample remains within the same limits that upon deformation. The density of dislocations is 3.3×10^{10} cm⁻², which is at the level of dislocation density values in unstrained sample. No changes were observed upon annealing in other crystal structure defects, such as twins and stacking faults.

Deformation vacancy clusters (DVC). According to work [5], upon deformation the examined steels contain more than 50 appm DV. Based on the data on the mobility of dislocations in these steels and high stability of vacancy clusters and considering the effect of multiplicity on the stability and size of DVC, the authors of work [5] make a conclusion about the size and concentration of DVC, which are respectively 0.6 nm and more than 10 appm.

2.2. Radiation-induced segregation of hydrogen

Hydrogen atoms are very labile and usually decorate defects. This occurs also in case of implantation of ions into hydrogen-containing target. Since the distribution of radiation defects in ion-irradiated target is not uniform, the distribution of hydrogen related to defects is not uniform either, i.e. radiation-induced segregation of hydrogen (RIS) takes place [6]. RIS arises also during implantation of hydrogen [7 - 10]. In the conditions when defects formed during implantation or their complexes with hydrogen atoms have small mobility, the region of enhanced hydrogen concentration (the region

of segregation or RIS) is localized in ion-irradiated volume. This volume is limited to a section of the ion beam, the surface and the length of the projected range of the implanted ion.

It is obvious that the data on the amount of trapped hydrogen and on its distribution in the depth provide information about the amount and nature of radiation-induced defects – hydrogen atom traps. Such information can be received by employing the following schemes.

1. RIS is generated by implanting beam of accelerated deuterium ions (deuterons) and is analyzed by accelerated helium ions by means of nuclear reaction $D(^3\text{He},p)^4\text{He}$ [11]. Both beams “work” simultaneously combining the ion irradiation and measuring processes in time.

2. RIS is generated and analyzed by one beam of accelerated deuterons (nuclear reaction $D(d,p)T$).

Each of these schemes has its own merits and demerits. The obvious advantage of both schemes is that all deuterium registered in the experiment is of implantation origin.

2.3. Nuclear reactions method

The unique prospects of using the reaction $D(d,p)T$ for measuring the concentration of deuterium in the real time of ion irradiation process have been repeatedly considered in the literature [13]. The small number of experimental works where this nuclear reaction is used is connected, in our opinion, with the ambiguous character of the obtained results and with the difficulty of their interpretation. Since with a decrease in the energy of deuterons entering into the nuclear reaction the energy of the formed protons increases, then, with allowance for deceleration of deuterons and protons in the target, the protons coming from different depths get in one spectrometer channel, i.e. there is an ambiguous dependence between the energy of the nuclear reaction products and the depth of analysis. By setting the detection angle of 120 degrees, i.e. considerably increasing the energy losses of protons, we managed to overcome partially this ambiguity. Using the sample with constant deuterium concentration, $\text{TiD}_{1.78}$, as a standard and selecting the optimal conditions for its irradiation and measuring, we obtained the information about the concentration of deuterium in irradiated material in the *in situ* mode.

The choice of the deuteron energy value in the reaction $D(d,p)T$ (700 keV), as opposed to numerous works where this energy does not exceed tens of keV, allowed us to expand the analysis region up to $\sim 4 \mu\text{m}$ (steels, iron, nickel) and thereby to take it way from the sample surface and concomitant impurities [11]. Besides, this approach provided the accuracy of the experiment with respect to introduction of additional component into the target (helium) and excluded the creation of radiation-damaged areas outside the deuterium implantation region.

The choice of irradiation, detection and calculation conditions [6] allowed us to determine from the energy spectrum of protons the average concentration of deuterium in irradiated volume C_D as a function of the implantation dose F . In the experiment, C_D was measured during continuous ion irradiation and discrete registration of the energy spectrum of reaction products – protons. All the experiments with the use of reaction $D(d,p)T$ were carried out at room temperature.

As distinct from heavier ions, during implantation of deuterium, its real distribution at room temperature differs essentially from the estimated values. Diffusion redistribution of deuterium takes place incompletely. Some implanted atoms (captured in traps) remain in irradiated volume. This phenomenon is characterized by trapping coefficient α . It is calculated as a fraction of all implanted deuterium remaining in the irradiated region in the moment of measuring, i.e. $\alpha = C_D / C_D^{theor} \times 100\%$, where C_D^{theor} is the average concentration of deuterium calculated on condition that all implanted atoms remain in the irradiated volume. It is evident that calculations with the SRIM software yield $\alpha = 1$, while for real distribution of implanted deuterium in irradiated material at 300 K $\alpha \ll 1$.

3. Results and discussion

3.1. Capture of deuterium in irradiated volume

The reason why implanted atoms partially remain in irradiated volume at temperatures providing diffusion redistribution of deuterium in the target is not only radiation-induced hydrogen traps in the radiation region (RIT), but also initial traps (IT). RIT are unevenly distributed in the depth of the radiation region (leading to RIS), whereas the distribution of IT in the target is uniform.

The elements of the microstructure of the examined steel identified as IT affect hydrogen capture in RIS both directly and indirectly (they can be point defect sinks). Hydrogen capture in the radiation damage region depends immediately on their total capacitance. If IT do not undergo evolution under irradiation, their capacitance during irradiation is a constant value.

Both single radiation-induced point defects and their clusters can be RIT. In the displacement cascades, vacancy clusters of cascade origin, VCc, can be formed. When radiation-induced structural phase transformations take place in the target under the action of radiation ([13]), the products of these transformations (precipitates of second phases) can also become RIT.

The dose dependence of total deuterium capture consists of dose dependences of capture on RIT and IT, i.e. $\alpha_{\text{tot}}(F) = \alpha_{\text{IT}}(F) + \alpha_{\text{RIT}}(F)$. At a relatively small density of RIT, when the fields of interaction of hydrogen traps do not overlap, $\alpha_{\text{RIT}}(F) \sim F$. If the capacitance of IT is denoted as Q_{IT} , after occupation of IT $\alpha_{\text{IT}}(F) = Q_{\text{IT}} / C_{\text{D}}^{\text{theor}}(F)$. Since $C_{\text{D}}^{\text{theor}} \sim F$, then $\alpha_{\text{IT}}(F) \sim 1/F$.

Analysis of total capture of implanted deuterium showed that there is a real possibility to separate the contributions to hydrogen capture by IT and RIT. So, at descending dependence $\alpha_{\text{o}}(F)$, the dependence $\alpha_{\text{IT}}(F)$ can be determined from its first points. Otherwise in the beginning of measuring the IT can be considered to be already filled, and for estimation of $\alpha_{\text{IT}}(F)$ the first point of the dependence $\alpha_{\text{o}}(F)$ should be used.

This approach makes it possible to determine the capacitance of each type of IT and their influence on the formation of RIT. In Figure 1, the results of examination of RIS in titanium-containing austenitic steel Kh16N15M3T1 are presented as an example [12].

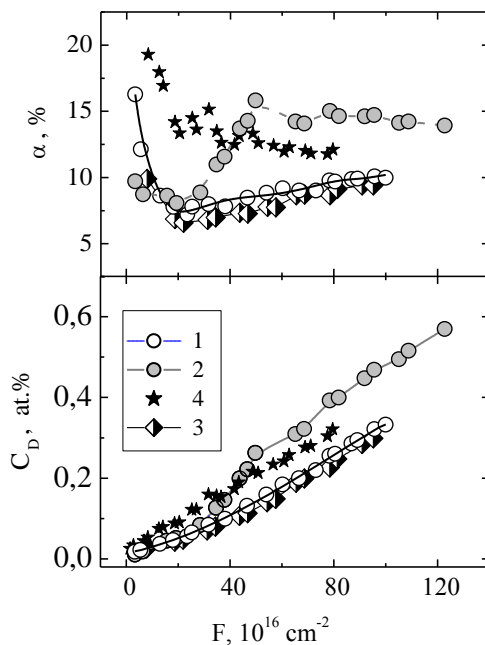


Figure 1. The effect of radiation dose F on C_{D} and α for Kh15N16M3T1 steel samples.

The numerals 1 - 4 denote samples ss11, ss11d, ss11do and ss11x, respectively.

Special preparation of the samples that provided a wide range of microstructures makes it possible to separate the contribution of each type of IT to total capture of implanted deuterium. So, for determination of the contribution of deformation vacancies to total deuterium capture, samples with the same dislocation density – after cold deformation without annealing and annealed sample – have been obtained. Samples with different dislocation density (hardened sample and sample annealed after deformation) were prepared to establish the trapping role of dislocations. In order to determine the

contribution of initial Ni_3Ti particles to total capture of implanted deuterium, along with hardened sample, we prepared an aged sample with Ni_3Ti particles. The capacitances of IT of the examined samples derived from $\alpha_{IT}(F)$ measurement results can be written as

$$Q^{ss01} = 0;$$

$$Q^{ss01d} = Q^{ss01}_{DV} + Q^{ss01}_{disl};$$

$$Q^{ss01do} = Q^{ss01}_{disl};$$

$$Q^{ss11} = Q_{TiC};$$

$$Q^{ss11d} = Q_{TiC} + Q^{ss11}_{DV} + Q^{ss11}_{disl};$$

$$Q^{ss11do} = Q_{TiC} + Q^{ss11}_{disl};$$

$$Q^{ss11x} = Q_{TiC} + Q_{Ni3Ti},$$

where Q^{ss01} is the total capacitance of IT of a sample of hardened titanium-free steel, which consists of capacitances of oxide inclusions and small-density dislocations. It is obvious that the mentioned structural elements are not effective deuterium traps. The DV, disl., TiC and Ni_3Ti indices are related respectively to deformation vacancy clusters, dislocations and titanium carbide TiC and Ni_3Ti particles.

Note that the $C_D(F)$ dependences of all the examined samples (Fig. 1a) are parallel lines when the implantation doses are greater than $50 \times 10^{16} \text{ cm}^{-2}$. Equal inclination of these dependences to the F axis shows that the RIT in all the samples are of one type, whereas different level of C_D values is indicative of the difference in the Q values. The total values of Q can be determined with a high degree of accuracy either from the initial area of dose dependences of total deuterium capture in RIS or from the ratio of Q values from $C_D(F)$ dependences.

The types of the initial traps and their capacitances Q obtained from analysis of $C_D(F)$ and $\alpha(F)$ and the results of TEM studies of the structure of the samples [2, 3] are listed in the Table. The asterisk * in the Table corresponds to Ni_3Ti particles formed during cold plastic deformation.

Table. Capture of implanted deuterium on initial traps in Kh16N15M3T1 steel

Sample	Capacitance of different types IT, appm				
	Q_{Σ}	Q_{TiC}	Q_{Ni3Ti}	Q_{disl}	Q_{DVC}
hardened	170	170	0	0	0
aged	770	170	600	0	0
strained	450	170	180*	250	30
annealed	420	170	165*	250	0

The fact that carbides are effective hydrogen traps agrees well with the results of work [14].

The total deuterium capture for all the examined samples was decomposed according to the scheme presented in Figure 2 for sample ss11 (hardened steel with titanium). The indices tot, IT, RIT and Ni_3Ti correspond to total deuterium capture, to capture on IT, RIT and radiation-induced particles of Ni_3Ti ($\alpha_{tot} = \alpha_{IT} + \alpha_{RIT}$ and $\alpha_{RIT} = \alpha_{VCc} + \alpha_{Ni3Ti}$). The notation VCc corresponds to deuterium capture on vacancy clusters of cascade origin. Since deuterium capture on IT in ss01 sample is absent, for this sample $\alpha_{tot} = \alpha_{RIT} = \alpha_{VCc}$.

Comparison of $\alpha_{RIT}(F)$ of Kh16N15M3(T1) steel samples revealed that high-density dislocations with coherent deformation-induced precipitates of Ni_3Ti are effective vacancy sinks. Radiation-

induced vacancies, in their turn, are building materials for effective RIT – vacancy clusters. The initial Ni_3Ti precipitates produced by aging of unstrained steel are also effective vacancy sinks and deuterium traps.

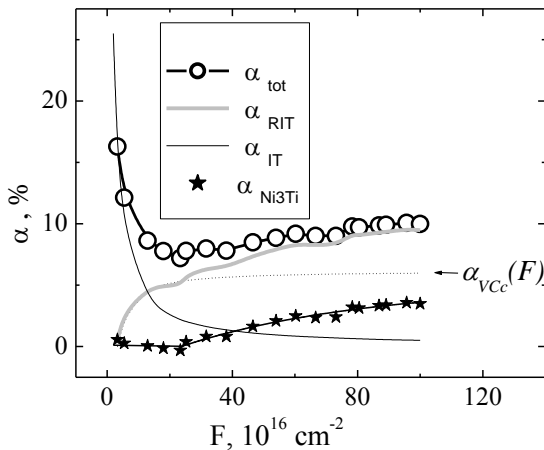


Figure 2. The scheme of decomposition of total deuterium capture α into trapping capture in hardened sample of steel Kh15N16M3T1

The efficiency of vacancy sinks manifests itself first of all in displacement of deuterium capture onset on VCc towards larger radiation doses. The implantation doses, at which deuterium capture on RIT begins, have been determined. For a hardened sample this dose is $\sim 3 \times 10^{16} \text{ cm}^{-2}$, and for ss11d, ss11do and ss11x samples it is $\sim 18 \times 10^{16} \text{ cm}^{-2}$.

4. Conclusions

1. The scheme employed in this work for studying radiation-induced segregation allowed us to separate the contributions from initial and radiation-induced traps to the total capture of implanted deuterium in irradiated volume. With special preparation of the initial structure of the samples, it has been possible to determine the type and capacitance of initial deuterium traps in them, as well as their effect on the number of traps appearing under irradiation.

2. It was found that cold deformation of steels at room temperature is accompanied by the formation of deuterium traps related to dislocations. Presumably, these traps, effectively capturing implanted deuterium, are precipitates (or rather pre-precipitates) of Ni_3Ti on dislocations.

3. It was shown that the initial traps (carbide particles, Ni_3Ti and clusters of strained vacancies) are effective sinks of vacancies that are mobile under experiment conditions. The quantity of clusters of radiation-induced vacancies decreases, and consequently implanted deuterium capture on radiation-induced traps lowers.

The work was done within RAS Program (project «Spin» № 012001463330, and «Flux» № 01201463334), with partial support of Russian Foundation for Basic Research (grant № 14-03-00359-a) and Ural Branch of RAS (grant № 15-17-2-3)

REFERENCES

- [1] Garner F A, Oliver B M, Greenwood L R, et al. 9th Meeting on environmental degradation of materials, Tahoe, Utah, august 2001 54–72
- [2] Arbuzov V L, Raspopova G A, Sagaradze V V, et al. 2004 *FMM* **97** No. 6 66–74 [in Russian]
- [3] Arbuzov V L, Raspopova G A, Sagaradze V B, et al. 2009 *FMM* **108** No. 1 81–92 [in Russian]
- [4] Raspopova G A, Arbuzov V L 2009 *Problems of atomic science and technology* Iss. 2 14-19
- [5] Druzhkov A P, Arbuzov V L, Perminov D A 2005 *J. Nucl. Mater.* **341** 153-163
- [6] Arbuzov V L, Vykhodetz V B, Raspopova G A 1995 *Fusion Technology* **28** 1127–31

- [7] Arbuzov V L, Raspopova G A, Danilov S E, et al. 2000 *J. Nucl. Mater.* **283-287** 849–853
- [8] Arbuzov V L, Raspopova G A 1999 *Advances in Science and Technology.* **24** 507–514
- [9] Raspopova G A, Arbuzov V L 2009 *Physics of Metals and Metallography* No. 107 58-67
- [10] Arbuzov V L, Raspopova G A 1999 *J. Nucl. Mater.* **271-272** 340–344
- [11] Neklyudov I M, Tolstolutsкая G D, et al. 2004 *Fizika i khimiya obrabotki materialov (Physics and chemistry of material working)* No. 2 50-55 [in Russian]
- [12] Kawachi N, Katabuchi T, Yamaguchi M and Tagishi Y 2002 *Nucl. Instr. and Meth.* **190** Iss. 1-4 195-198.
- [13] Borodin O V, Bryk V V, Voyevodin V N, Neklyudov I M 1999 *Metallofiz. noveishiye tekhnol. (Metal physics and high technologies)* **21** No. 6 51–65 [in Russian]
- [14] Zouev Yu N, Podgornova I V, Sagaradze V V 2000 *Fusion Engineering and Design* **49-50** 971–976